

Towards efficient and generic entanglement detection

Jue Xu* and Qi Zhao†

(Dated: October 20, 2022)

Detection of entanglement is an indispensable step to practical quantum computation and communication. Compared with existing works, we propose an end-to-end, machine learning assisted entanglement detection protocol that is more flexible and robust to different types of noises. In this protocol, an entanglement witness for a generic entangled state is obtained by classical machine learning with a synthetic dataset which consists of classical features of certain states and their labels. The classical features of a state, that is expectation values of a set of Pauli observables, are estimated by the sample-efficient scheme developed recently.

I. INTRODUCTION

Entanglement [1] is the key ingredient of quantum computation [2], quantum communication, and quantum cryptography [3]. However, decoherence and imperfection are inevitable in real-world devices, which means the interaction between a quantum system and classical environment would significantly affect entanglement quality and diminish quantum advantage. So, for practical purpose, it is essential to benchmark (characterize) entanglement structures of certain target states in actual (real) experiments. Though the entanglement detection problem [4] has been widely studied, it is far from being perfectly solved. Even we are given the full density matrix of a general state, it is computationally hard to determine its separability classically [5], even by quantum computation [6]. If we would like to know the separability of an unknown state from experiments, the sample complexity to fully recover a density matrix is prohibitive [7] [8]. So, a more realistic scenario is to determine whether a state from experiments is still entangled, assuming it is a known entangled state subject to noise. This problem for many entangled states of practical interest can be efficiently solved by measuring few observables called entanglement witness [9] [10] [11], but more analysis and measurement settings are required for more general states and noise cases [12] [13] [14].

The goal of this paper is to find an efficient and generic way to detect entanglement around a target state. Machine learning (ML) is a powerful tool for such purpose. As we know, many ML techniques including quantum machine learning models [15] have been proposed for classification tasks in physics, such as classification of phases and prediction of ground states [16] [17]. Entanglement detection as a typical classification problem has been studied by machine learning techniques, such as determining separability by Neural Network [18] [19] and deriving generic entanglement witness by Support Vector Machine [20] [21]. However, these prior machine learning assisted methods only consider the robustness to white noise and do not address the problem how to

efficiently extract classical features of quantum states in real experiments.

In contrast, our method exhibits better robustness to white noise than the conventional fidelity witness and also robust to coherent noise which is more realistic in experiments but not widely studied. Specifically, our protocol starts from evaluation of expectations of n -qubit Pauli observables of a target state. The set of expectation values that serves as classical features of the target state, together with its label, consist of a data point in a dataset. Then, a classical ML classifier is obtained by training with this dataset. With the trained classifier at hand, it is expected that brand new samples from real experiments can be classified with high accuracy, where classical features of quantum states are estimated by the classical shadow method [22] with affordable samples complexity.

This paper is organized as follows: in Section II, we briefly present necessary definitions about entanglement structures and mainstream entanglement detection methods; Section III demonstrates our end-to-end protocol including two parts: learning an entanglement witness from synthetic data and estimating classical features of states from experiments; at last, numerical simulation results are discussed in Section IV.

II. PRELIMINARIES

A. Entanglement structures

Large scale entanglement involving multiple particles maybe the main resource for quantum advantages in quantum computation and communication. Roughly, we say a quantum state ρ of n subsystems is *entangled* if it is not fully separable, i.e., the state cannot be written as the tensor product of all subsystems as $\rho = \rho_1 \otimes \cdots \otimes \rho_n$. However, the simple statement ‘the state is entangled’ would allow that only two of the particles are entangled while the rest is in a product state, which is very weak entanglement. So, the more interesting entanglement property is bipartite separability:

Definition 1 (bi-separable). A pure state $|\psi\rangle$ is bipartite separable (bi-separable) if and only if it can be written as a tensor product form $|\psi\rangle_{\text{bi}}^P = |\phi_A\rangle \otimes |\phi_B\rangle$

* juexu@cs.umd.edu

† zhaoqi@cs.hku.hk

with some bi-partition $\mathcal{P} = \{A, B \equiv \bar{A}\}$. A mixed state ρ is bi-separable if and only if it can be written as a convex combination of pure bi-separable states, i.e., $\rho_{\text{bi}} = \sum_i p_i |\psi_i\rangle\langle\psi_i|_{\text{bi}}^{\mathcal{P}_i}$ [23] with a probability distribution $\{p_i\}$. The set of all bi-separable states is denoted as \mathcal{S}_{bi} .

Definition 2 (GME). On the contrary, if a state ρ is not a convex combination of any (partition) bi-separable states, i.e., $\rho \notin \mathcal{S}_{\text{bi}}$, it possesses genuine multipartite entanglement (GME).

GME implies that all subsystems are indeed entangled with each other, so it is the strongest form of entanglement. Whereas, there is another restricted way for generalizing bi-separability to mixed states: if it is a mixing of pure bi-separable states with the same partition \mathcal{P}_2 , and we denote the state set as $\mathcal{S}_{\text{bi}}^{\mathcal{P}_2}$. It is practically interesting to study entanglement structure under certain partition, because it naturally indicates the quantum information processing capabilities among a real geometric configuration. We have a definition concerning partitions:

Definition 3 (full entanglement). A state ρ possesses full entanglement if it is outside of the separable state set $\mathcal{S}_{\text{bi}}^{\mathcal{P}_2}$ for any partition, that is, $\forall \mathcal{P}_2 = \{A, \bar{A}\}, \rho \notin \mathcal{S}_{\text{bi}}^{\mathcal{P}_2}$.

For a state with full entanglement, it is possible to prepare it by mixing bi-separable states with different bipartitions, so full entanglement is weaker than GME but still useful.

B. Entanglement detection

After introducing the definitions about entanglement, the next basic question is how to determine entanglement and its computational complexity. Despite its clear definitions, it is a highly non-trivial problem for a general state. For a general review on this subject, we refer readers to [4]. The most widely studied problem in this area maybe bi-separability.

Problem 1 (separability). Given a density matrix [24] ρ , to determine if it is bi-separable (in \mathcal{S}_{bi}).

It is not hard to prove that if a state is bi-separable regarding $\mathcal{P} = \{A, B\}$, then it must have positive partial transpose [25] (PPT), that is, the partially transposed (PT) density matrix $\rho_{AB}^{\text{T}_A}$ is positive, semidefinite [26] [27] [28]. By contrapositive, we have a sufficient condition for (bipartite) entanglement, that is

Theorem 1 (PPT criterion). *If the smallest eigenvalue of partial transpose $\rho_{AB}^{\text{T}_A}$ is negative (NPT), then the state is entangled (cannot be bi-separable with \mathcal{P}).*

We should mention that PPT criterion is a necessary and sufficient condition for separability only when the system dimension is low ($d_A d_B \leq 6$). [28]. Therefore, no general solution for the separability problem is

known. Then, a natural question is whether it is possible to solve separability approximately. By relaxing the definition (promise a gap between two types of states), a reformulation of separability in the theoretic computer science language is

Problem 2 (Weak membership problem for separability). Given a density matrix ρ with the promise that either (i) $\rho \in \mathcal{S}_{\text{bi}}$ or (ii) $\|\rho - \rho_{\text{bi}}\| \geq \epsilon$ with certain norm [29], decide which is the case.

Unfortunately, even we are given the complete information about a state and promised a gap (error tolerance ϵ), it is still hard to determine separability approximately by classical computation. **Weak membership problem for separability** is NP-Hard for $\epsilon = 1/\text{poly}(D)$ with respect to Euclidean norm and trace norm [5]. [30] [31] while there exists a quasipolynomial-time algorithm with respect to $\|\cdot\|_{\text{LOCC}}$ (and $\|\cdot\|_2$?) [32]. quantum hardness ... [6] A notable example is the widely-used and powerful criteria called k -symmetric extension hierarchy based on SDP [33], which is computationally intractable with growing k . Nevertheless, these hardness results do not rule out the possibility to solve it efficiently with stronger promise (approximation) or by machine learning (heuristic) techniques powered by data.

1. Entanglement witness based on fidelity

A related but different problem setting is how to determine bi-separable given copies of an unknown state (from experiments) rather than its density matrix. Since the input to this problem is quantum data (states), directly estimating spectrum of the reduced density matrix $\rho_A := \text{Tr}_B(\rho_{AB})$ by quantum circuits is a good option (without fully recovering density matrix). For example, multivariate trace $\text{Tr}(\rho_A^m)$ encodes the entanglement information (e.g., purity, negativity, and entanglement entropy) of ρ_{AB} with ρ_A being the reduced density matrix $E(\Psi_{AB}) := S(\rho_A) = -\text{Tr}(\rho_A \log \rho_A)$ [34] [35] [36]. The multivariate trace can be estimated by constant depth quantum circuits [37] [38], but this line of work is still based on PPT criterion (not iff). The problem we study in this paper is another variant:

Problem 3 (entanglement detection). Given an unknown state ρ (from experiments) is promised either (i) $\rho \in \mathcal{S}_{\text{bi}}$ or (ii) in proximity of a target $|\psi_{\text{tar}}\rangle$ (i.e., possesses ‘useful’ entanglement such as GME, full entanglement, depth ...) [39], determine which is the case.

The typical scenario for this problem is one aims to prepare a pure entangled state $|\psi_{\text{tar}}\rangle$ in experiments and would like to detect (verify) it as true multipartite entangled. While the preparation is not perfect, it is reasonable to assume that the prepared mixed state ρ_{pre} is in the proximity of the target state, that is, $|\psi_{\text{tar}}\rangle$ undergoes noise channels restricted to white noise, bit/phase-flip error, or random local unitary.

This problem can be expected to be solved more efficiently, because we have a much stronger promise than the [separability](#) problem. The usual method is constructing an observable W called entanglement witness such that

$$\text{Tr}(W\rho_{\text{bi}}) \geq 0 \text{ and } \text{Tr}(W|\psi_{\text{tar}}\rangle\langle\psi_{\text{tar}}|) < 0 \quad (1)$$

Eq. (1) means that the witness W has a positive expectation value on all separable states, hence a negative expectation value implies the presence of entanglement (GME). For every entangled state, a witness can always be constructed, but no entanglement witness works for all entangled states [40]. For example, the Bell (CHSH) inequalities originally proposed to rule out local hidden variable models, can be regarded as an entanglement witness [41]. A Bell inequality is a linear combination of Pauli observables $W_{\text{Bell}} := \mathbf{w}_{\text{Bell}} \cdot \mathbf{O}_{\text{Bell}}$ such that only entangled states ρ have $|\text{Tr}(\rho W_{\text{Bell}})|$ greater than a threshold [42].

While various methods for constructing an entanglement witness exist, the most common one is based on the fidelity between a prepared state ρ_{pre} to the target (pure entangled) state $|\psi_{\text{tar}}\rangle$

$$W_{\psi} = \alpha \mathbb{1} - |\psi_{\text{tar}}\rangle\langle\psi_{\text{tar}}| \quad (2)$$

where $\alpha = \max_{\rho_{\text{bi}}} \text{Tr}(\rho_{\text{bi}} |\psi_{\text{tar}}\rangle\langle\psi_{\text{tar}}|)$ is the smallest constant such that for every separable state $\text{Tr}(\rho_{\text{bi}} W) \geq 0$. For instance, assume the target state is $|\text{GHZ}\rangle := \frac{1}{\sqrt{2}}(|0\rangle^{\otimes n} + |1\rangle^{\otimes n})$, the maximal overlap between GHZ and bi-separable states is $1/2$, such that the witness Eq. (2) with $\alpha = 1/2$ certifies tripartite entanglement [43]. We call Eq. (2) as projector-based fidelity witness [9]. In order to effectly measure a witness in an experiment, it is preferable to decompose the projector term into a sum of locally measurable observables [44]. Moreover, for graph states (stabilizer states, i.e., a large class of entanglement states), a witness can be constructed by very few local measurement settings (tradeoff between robustness and meaurement efficiency) [10] [11] [45], while for non-stabilizer cases (e.g., W state), more careful analysis is required [14] [20]. Related experiments: photonic implementation with a few qubits (generation, verification) [46]; fully entangled graph state (ring of 16 qubits) IBM by measuring negativity [47]; optical lattice (homogeneous, restricted measurement, detect GME, nonstabilizer) [48];

III. END-TO-END ENTANGLEMENT DETECTION PROTOCOL

A. Motivation: Beyond fidelity witness

In most studies, the robustness measure of a fidelity witness is its tolerance (robustness) to white noise:

$$\rho = (1 - p_{\text{noise}}) |\psi_{\text{tar}}\rangle\langle\psi_{\text{tar}}| + p_{\text{noise}} \frac{\mathbb{1}}{2^n} \quad (3)$$

where the limit of (maximal) p_{noise} indicates the robustness of the witness. For example, the maximally-entangled Bell state can maximally violate the CHSH inequality, but Bell states mixed with white noise don't violate the CHSH inequality when $1 - 1/\sqrt{2} < p_{\text{noise}} < 2/3$, despite they are still entangled in this regime.

For 3-qubit GHZ and W states mixed with white noise, we can analytically compute the white noise threshold for NPT (implies bipartite entanglement): when $p_{\text{noise}} < 0.8$ (0.791 W), GHZ states cannot be [bi-separable](#) with respect to any partition (that is [full entanglement](#)). However, the conventional fidelity witness only detects [GME](#) when $p_{\text{noise}} < 4/7$ (8/21)[4]. So, it would be practically interesting to have a witness for this white noise regime.

Other than white noise, more realistic noise happened in (photonic) experiments is coherent noise, e.g., local rotations. Take GHZ state as an example, unconscious phase accumulation and rotation on the first control qubit can be modeled as [13]

$$|\text{GHZ}(\phi, \theta)\rangle = \cos \theta |0\rangle^{\otimes n} + e^{i\phi} \sin \theta |1\rangle^{\otimes n}. \quad (4)$$

In certain noise regime (see Fig. 3 in [13]), $|\text{GHZ}(\phi, \theta)\rangle$ cannot be detected by conventional fidelity witness because coherent noises diminish the fidelity but not change entanglement property.

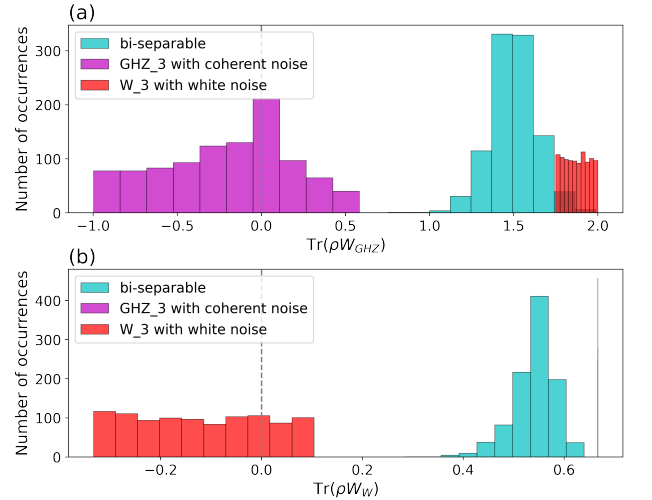


FIG. 1: Entanglement cannot be detected by fidelity witness GHZ state with coherent noise sampled $\theta \in [0, 0.5]$ and $\phi \in [0, 0.7]$; W state with large white noise. (a) GHZ projector fidelity witness (b) W projector fidelity witness

To formally characterize the cases beyond fidelity witness, Weilenmann et. al [49] coined the term *unfaithful states* which systematically analyze 2-qudit entangled state mixed with white noise that cannot be detected by fidelity witness. They found that for $d \geq 3$ that almost all states in the Hilbert space are unfaithful. Subsequently, G  the et. al [50] [51] give a formal definition: A 2-qudit state ρ_{AB} is faithful if and only if there are local unitary

transformations U_A and U_B such that

$$\langle \phi^+ | U_A \otimes U_B \rho_{AB} U_A^\dagger \otimes U_B^\dagger | \phi^+ \rangle > \frac{1}{d}. \quad (5)$$

Consequently, they found a necessary and sufficient condition for 2-qubit unfaithfulness, determined by the spectrum of

$$\mathcal{X}_2(\rho_{AB}) = \rho_{AB} - \frac{1}{2}(\rho_A \otimes \mathbb{1} + \mathbb{1} \otimes \rho_B) + \frac{1}{2}\mathbb{1} \otimes \mathbb{1}, \quad (6)$$

i.e., a 2-qubit state ρ_{AB} is faithful if and only if the maximal eigenvalue of $\mathcal{X}_2(\rho_{AB})$ is larger than $1/2$. We can see in Fig. 2, even for 2-qubit systems, nonnegligible portion of states are unfaithful but still entangled (NPT).

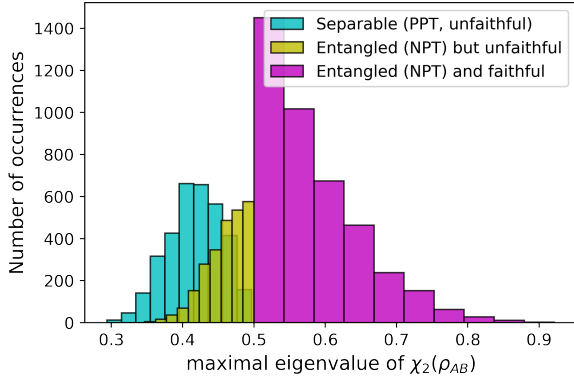


FIG. 2: Unfaithfulness of 2-qubit states determined by the maximal eigenvalue of Eq. (6).

Although there are variants of witness [13], such as nonlinear witness [12] and post-processing [52], designed to remedy the shortcomings of conventional fidelity witness respectively, it would be meaningful in practice to find a generic method to construct witnesses for **entanglement detection**. Machine learning techniques satisfy the needs well because supervised learning can be regarded as a powerful nonlinear post-processing tool.

B. Training a generic witness via SVM

The basic task of classical machine learning (ML) is the binary classification, such as cat/dog images classification. In this case (supervised learning), the input to a ML algorithm is a (training) dataset $\{(\mathbf{x}^{(i)}, y^{(i)})\}_{i=1}^m$ consists of m data points, where each is a pair of feature vector $\mathbf{x} \in \mathbb{R}^d$ of d features and its label (scalar) y (either -1 or 1). For example, the feature \mathbf{x} of an image is a flatten vector of all pixel values and the label $y = -1$ for cat (1 for dog). The classification problem can be formulated as a convex optimization problem: find a hyperplane \mathbf{w} (a linear function) such that maximize the margin between two partitions (see Fig. 3)

$$\max_{\mathbf{w}} \|\mathbf{w}\|^2 \text{ s.t. } \forall i, y^{(i)} \cdot (\mathbf{w} \cdot \mathbf{x} + b) \geq 1. \quad (7)$$

So, the prediction label is given by the sign of the inner product (projection) of the hyperplane and the feature vector, $y = \text{sign}(\mathbf{w} \cdot \mathbf{x} + b)$. It is clear to see **separability** or **entanglement detection** are exactly such binary classification problems where each quantum state has a binary label, such as **entangled/bi-separable**. The features \mathbf{x} of a quantum state ρ can be the entries of its density matrix, or more realistically, the expectation values of certain observables.

With the surge of ML research, ML algorithms have been proposed for classification tasks related to entanglement. Lu et. al [18] trained a (universal) **separability** classifier by classical neural network where features are the entries of density matrices. For the similar purpose, Ma and Yung [19] generalized Bell inequalities to a Bell-like ansatz $W_{\text{ml}} := \mathbf{w}_{\text{ml}} \cdot \mathbf{O}_{\text{Bell}}$ where the optimal weights \mathbf{w}_{ml} are obtained via a neural network. And they found the tomographic ansatz

$$W_{\text{ml}} := \mathbf{w}_{\text{ml}} \cdot \mathbf{O}_{\sigma}, \quad \forall \sigma \in \{I, X, Y, Z\}^n \quad (8)$$

where \mathbf{O}_{σ} is a vector of all 4^n Pauli observables [53], not only has better performance, also required [54] for a universal **separability** classifier. It is worth noting that training such a universal classifier for high-dimensional systems is hard if the gap between two state sets is small (weak promise).

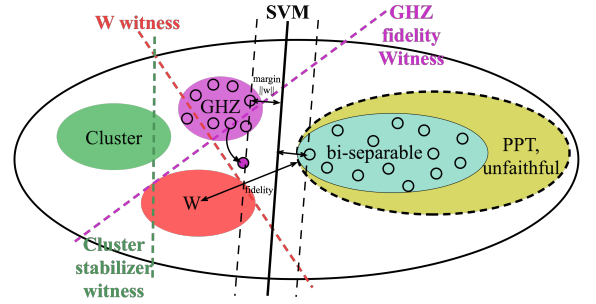


FIG. 3: Schematic diagram for entanglement detection methods: entanglement witnesses for different states are depicted by colored dash lines (hyperplane). SVM with the linear kernel (hyperplane). **PPT criterion** (non-linear, one-side) ...

In our paper, we focus on the problem **entanglement detection** with training data. In other words, we derive the entanglement witness for certain target states with desired entanglement structure by fitting a synthetic dataset.

Problem 4 (learn an entanglement witness). learn a witness for **entanglement detection** of ρ from data

- **Input:** a synthetic dataset consist of density matrices ρ with corresponding labels y
- **Output:** a classifier $f_{\text{ml}}(\mathbf{x})$ with high accuracy

The **learn an entanglement witness** problem has also been studied by classical ML [20] [21], but by a different technique called Support Vector Machine (SVM) [55].

The features $\mathbf{x} := \text{Tr}(\rho O_\sigma)$ of a state is a vector of expectations of Pauli observables. An SVM constructs a hyperplane $\langle W_{\text{svm}} \rangle = \mathbf{w}_{\text{svm}} \cdot \mathbf{x}$ that clearly delineates two kinds of states, see Fig. 3. Both SVM witness and conventional fidelity witness is a weighted sum of observables (features) which represents a hyperplane in the state (feature) space. The SVM witness is more flexible because coefficients are optimized (automatically derived) from training for any generic target state. This method only requires local (Pauli) measurements even when the target state is a non-stabilizer state, such as W state (normally need nonlocal measurements).

Algorithm III.1: train a witness via kernel SVM

input : states with labels: $\{(\rho^{(i)}, y^{(i)})\}_{i=1}^m$
output: a classifier $\mathbf{w}_{\text{ml}}, \sigma_{\text{ml}}$

```

1 Evaluate Pauli observables  $\mathbf{x}_{\rho, \sigma}^{(i)} := \text{Tr}(\rho^{(i)} O_\sigma), \forall i$ 
2 for  $j = 1, 2, \dots, 4^n$  do
3   while accuracy < 0.999 do
4     randomly select  $j$  features  $\tilde{\mathbf{x}}_i$  from  $\mathbf{x}_i, \forall i$ 
5     accuracy, classifier = SVM( $\{(\tilde{\mathbf{x}}^{(i)}, y^{(i)})\}_i^m$ )
6   return classifier  $\mathbf{w}_{\text{ml}}$ 
```

A key drawback (constraint) of conventional witnesses is its linearity. Despite the non-linear witness [12] proposed, its implementation in experiments is more challenging than linear one. The good news is, within the framework of SVM, non-linearity can be easily achieved by the kernel method [56]. The Gaussian (RBF) kernel $k_{\text{gaus}}(\mathbf{x}, \mathbf{x}') := \exp(-\gamma \|\mathbf{x} - \mathbf{x}'\|_2^2)$ with an infinite dimensional feature map $\phi(\mathbf{x})$. Fortunately, there is a very useful tool called kernel method or kernel trick to remedy this drawback. The main idea is mapping the features to a higher dimensional space such that they can be linearly separated in the high dimensional feature space. In general, the kernel function $k : \mathcal{X} \times \mathcal{X} \rightarrow \mathbb{R}$ measures the similarity between two input data points by an inner product.

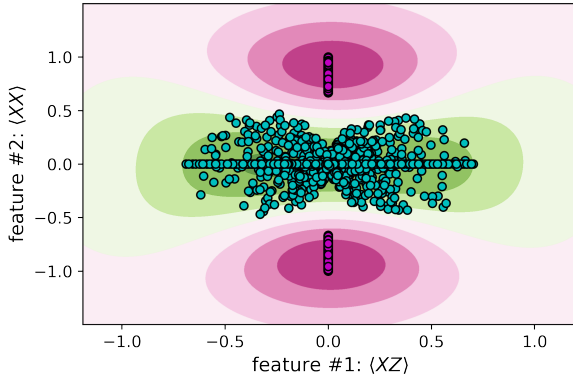


FIG. 4: two-dimensional embedding (feature space): green dots represent the separable states, while pink one represent entangled Bell states mixed with white noise.

We focus on kernel methods rather than neural networks (also non-linear), not only because of its clear geometric interpretation, but also its equivalence to neural network in terms of neural tangent kernel [57]. The advantages of SVM: (1) the training of an SVM is convex; if a solution exists for the given target state and ansatz, the optimal SVM will be found. (2) this SVM formalism allows for the programmatic removal of features [58], i.e., reducing the number of experimental measurements and copies (samples).

	# observables	weights	promise
fidelity witness	few local	fixed	strongest
Bell (CHSH) inequality	constant	fixed	weak
tomographic classifier	$4^n - 1$	trained	weakest
SVM (kernel) witness	$\ll 4^n - 1$	trained	strong

TABLE I: Comparison of CHSH inequality, fidelity witness, and ML witness ansatz.

However, these prior ML witnesses only consider the robustness to white noise and cannot be directly applied to experiments. In numerical simulation, we can efficiently evaluate classical features by direct calculation, but, in actual experiments, entries of a density matrix are not explicitly known. Instead, we need to estimate the observables by many measurements, which we will discuss in next section.

C. Sample-efficient expectation estimation methods

The brute force approach to fully characterize a state in an experiment is quantum state tomography [59] [60]. With a recovered density matrix, we can directly calculate classical features or separability measures, but full tomography is experimentally and computationally demanding. Even if adaptive or collective measurements (and post-processing) allowed [61], rigorous analysis [7] [8] show that $\Omega(D^2/\epsilon^2)$ measurements (copies?) are required for recovering a $D \times D$ density matrix with error tolerance ϵ measured in trace distance.

Now that full tomography is not practical for large systems, a workaround is to extract information about a state without fully recovering it. Since many interesting properties of a quantum system are often linear functions of the underlying density matrix ρ , such as classical features $x_{\rho, \sigma} = \text{Tr}(\rho O_\sigma)$ for entanglement witness [62], this enables the possibility to *shadow tomography* [63].

Problem 5 (shadow tomography). Aaronson's formulation ($\mathbb{P}[E_i \text{ accept } \rho] = ? \text{Tr}(E_i \rho)$)

- **Input:** copies of an unknown D -dimensional state ρ and M known 2-outcome measurements $\{E_1, \dots, E_M\}$
- **Output:** estimate $\mathbb{P}[E_i \text{ accept } \rho]$ to within additive error $\epsilon, \forall i \in [M]$, with $\geq 2/3$ success probability.

Though it is proved that [shadow tomography](#) can be implemented in a samples-efficient (copies) manner, $\tilde{O}(\log^4 M \cdot \log D \cdot \epsilon^{-4})$ copies [63] [64], Aaronson's shadow tomography procedure is very demanding in terms of quantum hardware. So, Huang et. al [22] introduce classical shadow (CS) method that is more friendly to experiments. In our pipeline, we focus on the classical shadow method and its variants.

A classical shadow is a succinct classical description of a quantum state, which can be extracted by performing reasonably simple single-copy measurements on a reasonably small number of copies of the state. The classical shadow attempts to approximate this expectation value by an empirical average over R independent samples, much like Monte Carlo sampling approximates an integral.

$$o_i = \text{Tr}(O_i \rho_{\text{CS}}) \text{ obeys } \mathbb{E}[o] = \text{Tr}(O_i \rho) \quad (9)$$

classical shadows are based on random Clifford measurements and do not depend on the structure of the concrete witness in question. In contrast, direct estimation crucially depends on the concrete witness in question and may be considerably more difficult to implement.

Algorithm III.2: estimate features by CS

input : samples of ρ and $O_{\sigma_{\text{ml}}}$
output: estimation of $\mathbf{x}_{\rho, \sigma_{\text{ml}}} := \text{Tr}(\rho O_{\sigma_{\text{ml}}})$

```

1 for  $i = 1, 2, \dots, R$  do
2    $\rho \mapsto U \rho U^\dagger$  // apply a random unitary
3    $|b\rangle \in \{0, 1\}^n$  // measurement outcome
4    $\rho_{\text{CS}} = \mathcal{M}^{-1}(U^\dagger |b\rangle\langle b| U)$  //  $\mathcal{M}$  quantum channel
5  $\text{CS}(\rho, R) = \{\rho_{\text{CS}_1}, \dots, \rho_{\text{CS}_R}\}$  // classical shadow
   // estimate features for SVM from classical shadow
6 return  $\mathbf{x}_{\rho, \sigma_{\text{ml}}} = \text{MEDIANOFMEANS}(\text{CS}(\rho, R) \sigma_{\text{ml}})$ 
```

Given a quantum state ρ , a classical shadow is created by repeatedly performing a simple procedure: Apply a unitary transformation $\rho \mapsto U \rho U^\dagger$, and then measure all the qubits in the computational basis $|b\rangle \in \{|0\rangle, |1\rangle\}^{\otimes n}$. Its classical shadow (snapshots) ρ_{CS} (a density matrix) can be reconstructed

$$\rho_{\text{CS}} := \mathcal{M}^{-1}(U^\dagger |b\rangle\langle b| U) \quad (10)$$

where \mathcal{M} is a quantum channel that depends on the ensemble of random unitary transformation... . The algorithm is summarized in Algorithm. III.2. The number of times this procedure is repeated is called the size of the classical shadow. Classical shadows with size of order $\log(M)$ suffice to predict M target functions $\{O_1, \dots, O_M\}$. The classical shadow size required to accurately approximate all reduced k -body density matrices scales exponentially in subsystem size k $\Omega(\log(M) 3^k / \epsilon^2)$ [22], but is independent of the total number of qubits n . [65]

The derandomized variant of classical shadow [66] is the refinement of the original randomized protocol, but not necessarily guarantees better performance for global

observables (involving all subsystems). noise-resilient variant [67] ... experiments of classical shadow and related comparison [68]; detect entanglement by estimating p_3 -PPT with classical shadow [69]. The task of estimating expectation value can also be achieved efficiently by machine learning with training data [70] [71] [72] [17] [73]. Huang et. al rigorously show that, for any quantum process \mathcal{E} , observables O , and distribution \mathcal{D} , and for any quantum ML model, one can always design a classical ML model achieving a similar average prediction error such that N_C (number of experiments?) is larger than N_Q by at worst a small polynomial factor. In contrast, for achieving accurate prediction on all inputs $\text{Tr}(\rho O_\sigma), \forall \sigma \in \{I, X, Y, Z\}^n$, exponential quantum advantage is possible. [74] [75] [76]

IV. NUMERICAL SIMULATION

A. Dataset preparation and states generation

We generate quantum state samples, construct quantum circuits, and manipulate quantum objects numerically by QuTiP library [77] [78]. We generate multipartite entangled states (synthetic data) including: Bell states, 3-qubit GHZ and W states, 4-qubit graph (1D cluster) state, see Fig. 5 for examples. In contrast to en-

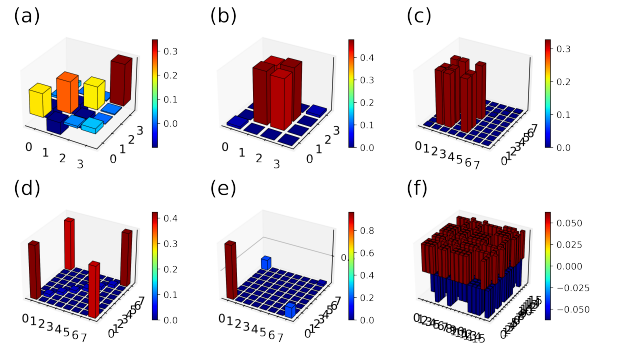


FIG. 5: Data preparation (real part): (a) random 2-qubit density matrix; (b) Bell state with white noise; (c) 3-qubit W state with white noise; (d) 3-qubit GHZ state with white noise; (e) GHZ state with coherent noise; (f) 4-qubit linear cluster, bi-separable state

tangled states, we generate random separable states for different number of qubits by tensoring random density matrices of subsystems. For example, 2-qubit: bipartite $\rho_A \otimes \rho_B$ where ρ_A and ρ_B are random density matrices (sampled by Haar measure); 3-qubit pure states: $\rho_A \otimes \rho_{BC}$, $\rho_C \otimes \rho_{AB}$, and $\rho_B \otimes \rho_{AC}$. For different noise channels: white noise according to Eq. (3), coherent noise according to Eq. (4).

B. Classification accuracy and comparison

For the machine learning part, we make use of scikit-learning package [79] to train SVM with the radial basis function (RBF) kernel.

Fig. 4 shows the two-dimensional embedding of 2-qubit states (feature space). The colored shade indicates the decision boundary of our trained classifier (ML witness), which exhibits that two kinds of data points are clearly classified.

Fig. 6 shows that the SVM witness can classify the states that cannot be detected by conventional fidelity witness, where the noise is randomly (uniform) sampled from $[0, p_{\text{noise}}]$.

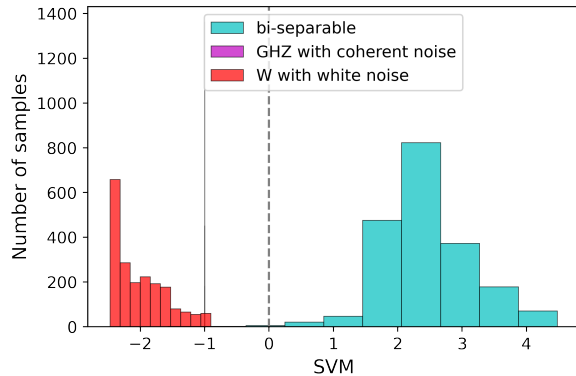


FIG. 6: ML witness for the states cannot be detect by fidelity witness (GHZ state with coherence noise, and W state with large white noise)

dataset size for training: 10^3 for 3-qubit case; more qubits [TODO]...

V. CONCLUSION AND DISCUSSION

Related experiments: our protocol is more flexible (a subset of observables which are realistic in experiments), but no guarantee (need more research) Possible directions for future research: (1) rigorous proof for dataset size and number of features (required for high training accuracy) scaling with the system size; (2) better kernel options such as graph kernel, quantum kernel, shadow kernel and neural tangent kernel; (3) quantum machine learning for estimating all classical features (tomography) efficiently; (4) if we have all classical features, is it possible to train a universal classifier or with weaker promise; (5) can we estimate concurrence... by quantum circuit; (6) quantum complexity for separability

ACKNOWLEDGMENTS

-
- [1] R. Horodecki, P. Horodecki, M. Horodecki, and K. Horodecki, *Rev. Mod. Phys.* **81**, 865 (2009), [arXiv:quant-ph/0702225](#).
 - [2] H. J. Briegel, D. E. Browne, W. Dür, R. Raussendorf, and M. V. den Nest, *Nature Phys* **5**, 19 (2009), [arXiv:0910.1116](#).
 - [3] F. Xu, X. Ma, Q. Zhang, H.-K. Lo, and J.-W. Pan, *Rev. Mod. Phys.* **92**, 025002 (2020), [arXiv:1903.09051](#).
 - [4] O. Gühne and G. Toth, *Physics Reports* **474**, 1 (2009), [arXiv:0811.2803 \[cond-mat, physics:physics, physics:quant-ph\]](#).
 - [5] L. Gurvits, *Classical deterministic complexity of Edmonds' problem and Quantum Entanglement* (2003), [arXiv:quant-ph/0303055](#).
 - [6] G. Gutoski, P. Hayden, K. Milner, and M. M. Wilde, *Theory of Comput.* **11**, 59 (2015), [arXiv:1308.5788 \[quant-ph\]](#).
 - [7] J. Haah, A. W. Harrow, Z. Ji, X. Wu, and N. Yu, *IEEE Trans. Inform. Theory*, 1 (2017).
 - [8] R. O'Donnell and J. Wright, in *Proc. Forty-Eighth Annu. ACM Symp. Theory Comput.* (ACM, Cambridge MA USA, 2016) pp. 899–912.
 - [9] M. Bourennane, M. Eibl, C. Kurtsiefer, S. Gaertner, H. Weinfurter, O. Guehne, P. Hyllus, D. Bruss, M. Lewenstein, and A. Sanpera, *Phys. Rev. Lett.* **92**, 087902 (2004), [arXiv:quant-ph/0309043](#).
 - [10] G. Toth and O. Guehne, *Phys. Rev. Lett.* **94**, 060501 (2005), [arXiv:quant-ph/0405165](#).
 - [11] G. Tóth and O. Gühne, *Phys. Rev. A* **72**, 022340 (2005).
 - [12] O. Gühne and N. Lütkenhaus, *Phys. Rev. Lett.* **96**, 170502 (2006).
 - [13] Y. Zhou, *Phys. Rev. A* **101**, 012301 (2020), [arXiv:1907.11495 \[quant-ph\]](#).
 - [14] Y. Zhang, Y. Tang, Y. Zhou, and X. Ma, *Phys. Rev. A* **103**, 052426 (2021), [arXiv:2012.07606 \[quant-ph\]](#).
 - [15] I. Cong, S. Choi, and M. D. Lukin, *Nat. Phys.* **15**, 1273 (2019), [arXiv:1810.03787 \[cond-mat, physics:quant-ph\]](#).
 - [16] J. Carrasquilla and R. G. Melko, *Nature Phys* **13**, 431 (2017), [arXiv:1605.01735](#).
 - [17] H.-Y. Huang, R. Kueng, G. Torlai, V. V. Albert, and J. Preskill, *Science* **377**, eabk3333 (2022), [arXiv:2106.12627](#).
 - [18] S. Lu, S. Huang, K. Li, J. Li, J. Chen, D. Lu, Z. Ji, Y. Shen, D. Zhou, and B. Zeng, *Phys. Rev. A* **98**, 012315 (2018), [arXiv:1705.01523 \[quant-ph\]](#).
 - [19] Y.-C. Ma and M.-H. Yung, *npj Quantum Inf* **4**, 34 (2018), [arXiv:1705.00813 \[quant-ph\]](#).

- [20] E. Y. Zhu, L. T. H. Wu, O. Levi, and L. Qian, *Machine Learning-Derived Entanglement Witnesses* (2021), [arXiv:2107.02301 \[quant-ph\]](#).
- [21] S. V. Vintskevich, N. Bao, A. Nomerotski, P. Stankus, and D. A. Grigoriev, *Classification of four-qubit entangled states via Machine Learning* (2022), [arXiv:2205.11512 \[quant-ph\]](#).
- [22] H.-Y. Huang, R. Kueng, and J. Preskill, *Nat. Phys.* **16**, 1050 (2020), [arXiv:2002.08953 \[quant-ph\]](#).
- [23] For different i , \mathcal{P}_i can be different partitions.
- [24] A quantum (mixed) state ρ can be represented by a density matrix which is a Hermitian, positive semidefinite operator (matrix) of trace one. If the rank of ρ is 1, then the state is a pure state.
- [25] The partial transpose (PT) operation - acting on subsystem A - is defined as $|k_A, k_B\rangle\langle l_A, l_B|^{\text{T}_A} := |l_A, k_B\rangle\langle k_A, l_B|$ where $\{|k_A, k_B\rangle\}$ is a product basis of the joint system \mathcal{H}_{AB} .
- [26] A matrix (operator) is positive, semidefinite (PSD) if all its eigenvalues are non-negative.
- [27] A. Peres, *Phys. Rev. Lett.* **77**, 1413 (1996), [arXiv:quant-ph/9604005](#).
- [28] M. Horodecki, P. Horodecki, and R. Horodecki, *Physics Letters A* **223**, 1 (1996), [arXiv:quant-ph/9605038](#).
- [29] Schatten p -norm $\|x\|_p := (\sum_i |x_i|^p)^{1/p}$. Euclidean norm l_2 norm; Spectral (operator) norm $\|x\|_\infty$; Trace norm $\|A\|_{\text{Tr}} \equiv \|A\|_1 := \text{Tr}(|A|) \equiv \text{Tr}(\sqrt{A^\dagger A})$, $|A| := \sqrt{A^\dagger A}$, $p = 1$; Correspondingly, trace distance between two density matrices is $d_{\text{tr}}(\rho, \rho') := \frac{1}{2}\|\rho - \rho'\|_1$. Uhlmann fidelity $F(\rho, \rho') := \text{Tr}(\sqrt{\sqrt{\rho}\rho'\sqrt{\rho}}) \equiv \|\sqrt{\rho}\sqrt{\rho'}\|_1$. linear fidelity or overlap $F(\rho, \rho') := \text{tr}(\rho\rho')$ fidelity and trace distance are related by the inequalities $1 - F \leq D_{\text{tr}}(\rho, \rho') \leq \sqrt{1 - F^2}$.
- [30] L. M. Ioannou, *Quantum Inf. Comput.* **7**, 335 (2007), [arXiv:quant-ph/0603199](#).
- [31] A. C. Doherty, P. A. Parrilo, and F. M. Spedalieri, *Phys. Rev. A* **69**, 022308 (2004), [arXiv:quant-ph/0308032](#).
- [32] F. G. Brandão, M. Christandl, and J. Yard, in *Proc. 43rd Annu. ACM Symp. Theory Comput. - STOC 11* (ACM Press, San Jose, California, USA, 2011) p. 343, [arXiv:1011.2751 \[quant-ph\]](#).
- [33] M. Navascués, M. Owari, and M. B. Plenio, *Phys. Rev. A* **80**, 052306 (2009), [arXiv:0906.2731 \[quant-ph\]](#).
- [34] A. K. Ekert, C. M. Alves, D. K. L. Oi, M. Horodecki, P. Horodecki, and L. C. Kwek, *Phys. Rev. Lett.* **88**, 217901 (2002), [arXiv:quant-ph/0203016](#).
- [35] P. Horodecki and A. Ekert, *Phys. Rev. Lett.* **89**, 127902 (2002), [arXiv:quant-ph/0111064](#).
- [36] The well-known identity (related to the replica trick originating in spin glass theory) $\text{Tr}(U^\pi(\rho_1 \otimes \dots \otimes \rho_m)) = \text{Tr}(\rho_1 \dots \rho_m)$ where the RHS is the multivariate trace and U^π is a unitary representation of the cyclic shift permutation.
- [37] S. Johri, D. S. Steiger, and M. Troyer, *Phys. Rev. B* **96**, 195136 (2017), [arXiv:1707.07658](#).
- [38] Y. Quek, M. M. Wilde, and E. Kaur, *Multivariate trace estimation in constant quantum depth* (2022), [arXiv:2206.15405 \[hep-th, physics:quant-ph\]](#).
- [39] For fidelity witness, promise that the state is either (1) fidelity $\|\rho_{\text{bi}} - |\psi_{\text{tar}}\rangle\langle\psi_{\text{tar}}|\| \geq \alpha$; (2) fidelity $< \alpha$ implies $\rho \in \mathcal{S}_{\text{bi}}$.
- [40] T. Heinosaari and M. Ziman, *The Mathematical Language of Quantum Theory: From Uncertainty to Entanglement*, 1st ed. (Cambridge University Press, 2011).
- [41] B. M. Terhal, *Physics Letters A* **271**, 319 (2000), [arXiv:quant-ph/9911057](#).
- [42] The CHSH inequality: $\mathbf{O}_{\text{CHSH}} = (\mathbb{1}, ab, ab', a'b, a'b')$ with $a = Z, a' = X, b = (X - Z)/\sqrt{2}, b' = (X + Z)/\sqrt{2}$ and $\mathbf{w}_{\text{CHSH}} = (\pm 2, 1, -1, 1, 1)$.
- [43] A. Acin, D. Bruss, M. Lewenstein, and A. Sanpera, *Phys. Rev. Lett.* **87**, 040401 (2001), [arXiv:quant-ph/0103025](#).
- [44] Such as $W_{\text{GHZ}_3} = \frac{1}{8}(3 * III - XXX - ZZI - ZIZ - IZZ + XYY + \dots)$ where $ZZI \equiv Z \otimes Z \otimes I$ for readability.
- [45] Y. Zhou, Q. Zhao, X. Yuan, and X. Ma, *npj Quantum Inf* **5**, 83 (2019).
- [46] H. Lu, Q. Zhao, Z.-D. Li, X.-F. Yin, X. Yuan, J.-C. Hung, L.-K. Chen, L. Li, N.-L. Liu, C.-Z. Peng, Y.-C. Liang, X. Ma, Y.-A. Chen, and J.-W. Pan, *Phys. Rev. X* **8**, 021072 (2018).
- [47] Y. Wang, Y. Li, Z.-q. Yin, and B. Zeng, *npj Quantum Inf* **4**, 46 (2018), [arXiv:1801.03782](#).
- [48] Y. Zhou, B. Xiao, M.-D. Li, Q. Zhao, Z.-S. Yuan, X. Ma, and J.-W. Pan, *npj Quantum Inf* **8**, 1 (2022).
- [49] M. Weilenmann, B. Dive, D. Trillo, E. A. Aguilar, and M. Navascués, *Phys. Rev. Lett.* **124**, 200502 (2020), [arXiv:1912.10056 \[quant-ph\]](#).
- [50] O. Gühne, Y. Mao, and X.-D. Yu, *Phys. Rev. Lett.* **126**, 140503 (2021), [arXiv:2008.05961 \[quant-ph\]](#).
- [51] G. Riccardi, D. E. Jones, X.-D. Yu, O. Gühne, and B. T. Kirby, *Exploring the relationship between the faithfulness and entanglement of two qubits* (2021), [arXiv:2102.10121 \[quant-ph\]](#).
- [52] Y. Zhan and H.-K. Lo, *Detecting Entanglement in Unfaithful States* (2021), [arXiv:2010.06054 \[quant-ph\]](#).
- [53] Denote $O_\sigma \in \{I, X, Y, Z\}^{\otimes n}$ for a Pauli observable. Denote $\mathbf{x}_{\rho, \sigma} := (\text{Tr}(\rho O_{\sigma_1}), \dots, \text{Tr}(\rho O_{\sigma_M}))$ for expectations of M Pauli observables with respect to the state ρ where $\sigma \subseteq \{I, X, Y, Z\}^n$.
- [54] D. Lu, T. Xin, N. Yu, Z. Ji, J. Chen, G. Long, J. Baugh, X. Peng, B. Zeng, and R. Laflamme, *Phys. Rev. Lett.* **116**, 230501 (2016), [arXiv:1511.00581 \[quant-ph\]](#).
- [55] C. Cortes and V. Vapnik, *Mach Learn* **20**, 273 (1995).
- [56] T. Hofmann, B. Schölkopf, and A. J. Smola, *Ann. Statist.* **36**, 10.1214/009053607000000677 (2008).
- [57] A. Jacot, F. Gabriel, and C. Hongler, *Neural Tangent Kernel: Convergence and Generalization in Neural Networks* (2020), [arXiv:1806.07572 \[cs, math, stat\]](#).
- [58] I. Guyon, J. Weston, S. Barnhill, and V. Vapnik, *Machine Learning* **46**, 389 (2002).
- [59] J. Altepeter, E. Jeffrey, and P. Kwiat, in *Advances In Atomic, Molecular, and Optical Physics*, Vol. 52 (Elsevier, 2005) pp. 105–159.
- [60] Quantum state tomography refers to the task of estimating complete description (recovering the density matrix) of an unknown D -dimensional state ρ within error tolerance ϵ , given the ability to prepare and measure copies of ρ .
- [61] Intermediate between independent measurements and unrestricted (also called “collective” or “entangled”) measurements are adaptive measurements in which the copies of ρ are measured individually, but the choice of measurement basis can change in response to earlier measurements.
- [62] Nonlinear functions: von Neumann entropy $\text{Tr}(\rho \log(\rho))$; multivariate functions: $\text{Tr}(\rho_1 \dots \rho_m)$, fidelity (quantum kernel?) $\text{Tr}(\rho\rho')$, quadratic $\text{Tr}(O\rho_i \otimes \rho_j)$.

- [63] S. Aaronson, in *Proc. 50th Annu. ACM SIGACT Symp. Theory Comput.*, STOC 2018 (Association for Computing Machinery, New York, NY, USA, 2018) pp. 325–338, [arXiv:1711.01053](#).
- [64] Full tomography: additive error $\epsilon \ll 1/D$.
- [65] Known fundamental lower bounds state that classical shadows of exponential size (at least) $T = \Omega(2^n/\epsilon^2)$ are required to ϵ -approximate ρ in trace distance.
- [66] H.-Y. Huang, R. Kueng, and J. Preskill, *Phys. Rev. Lett.* **127**, 030503 (2021), [arXiv:2103.07510 \[quant-ph\]](#).
- [67] S. Chen, W. Yu, P. Zeng, and S. T. Flammia, *PRX Quantum* **2**, 030348 (2021), [arXiv:2011.09636 \[quant-ph\]](#).
- [68] T. Zhang, J. Sun, X.-X. Fang, X.-M. Zhang, X. Yuan, and H. Lu, *Experimental quantum state measurement with classical shadows* (2021), [arXiv:2106.10190 \[physics, physics:quant-ph\]](#).
- [69] A. Elben, R. Kueng, H.-Y. Huang, R. van Bijnen, C. Kokail, M. Dalmonte, P. Calabrese, B. Kraus, J. Preskill, P. Zoller, and B. Vermersch, *Phys. Rev. Lett.* **125**, 200501 (2020), [arXiv:2007.06305 \[cond-mat, physics:quant-ph\]](#).
- [70] X. Gao and L.-M. Duan, *Nat Commun* **8**, 662 (2017), [arXiv:1701.05039 \[cond-mat, physics:quant-ph\]](#).
- [71] G. Torlai, G. Mazzola, J. Carrasquilla, M. Troyer, R. Melko, and G. Carleo, *Nature Phys* **14**, 447 (2018), [arXiv:1703.05334](#).
- [72] H.-Y. Huang, M. Broughton, M. Mohseni, R. Babbush, S. Boixo, H. Neven, and J. R. McClean, *Nat Commun* **12**, 2631 (2021), [arXiv:2011.01938 \[quant-ph\]](#).
- [73] Y. Zhu, Y.-D. Wu, G. Bai, D.-S. Wang, Y. Wang, and G. Chiribella, *Flexible learning of quantum states with generative query neural networks* (2022), [arXiv:2202.06804 \[quant-ph\]](#).
- [74] H.-Y. Huang, R. Kueng, and J. Preskill, *Phys. Rev. Lett.* **126**, 190505 (2021), [arXiv:2101.02464 \[quant-ph\]](#).
- [75] $\mathcal{O}(\log(M/\delta)\epsilon^{-4})$ copies of the unknown quantum state ρ . ($M = 4^n$ implies linear copy for full tomography??).
- [76] The required amount of training data scales badly with ϵ . This unfortunate scaling is not a shortcoming of the considered ML algorithm, but a necessary feature.
- [77] J. R. Johansson, P. D. Nation, and F. Nori, *Computer Physics Communications* **184**, 1234 (2013), [arXiv:1110.0573](#).
- [78] B. Li, S. Ahmed, S. Saraogi, N. Lambert, F. Nori, A. Pitchford, and N. Shammah, *Quantum* **6**, 630 (2022), [arXiv:2105.09902 \[quant-ph\]](#).
- [79] F. Pedregosa, G. Varoquaux, A. Gramfort, V. Michel, B. Thirion, O. Grisel, M. Blondel, P. Prettenhofer, R. Weiss, V. Dubourg, J. Vanderplas, A. Passos, D. Cournapeau, M. Brucher, M. Perrot, and É. Duchesnay, *J. Mach. Learn. Res.* **12**, 2825 (2011).